Structure resolution

Imaging light atoms by X-ray holography

We demonstrate here the imaging of light atoms by hard X-ray holography. Using intense synchrotron radiation for the excitation, the oxygen and nickel atoms in a nickel oxide sample are imaged in three dimensions with high resolution inside a volume of about 1,000 cubic ångströms. These remarkable characteristics mean that X-ray holography bridges the gap between diffraction, which relies on long-range order, and extended X-ray absorption fine structure, which gives information on the local environment of atoms.

For atomic resolution in solids by hard X-ray holography, selected atoms in the sample serve as reference points and their local environments are holographically imaged[1–3]. After holographic reconstruction, the intensity of the atoms is proportional to the square of their atomic number (z) and also to r^{-2}, where r is the distance from the central atom. To see an atom with a low value of z or at a large distance from the reference, the holographic oscillations therefore have to be measured with great precision.

To achieve this precision, we have used synchrotron radiation and a sophisticated experimental set-up[4,5], carrying out our measurements at the two undulator beamlines ID 32 and ID 22 of the European Synchrotron Radiation Facility. To avoid the twin images inherent in the traditional holographic type of reconstruction, which can distort the three-dimensional real-space image[6], we collected holograms at eight different energies (from 16.4 to 19.9 keV, in 0.5-keV steps)[3,7].

For data handling[4], we incorporated background subtraction, deconvolution of the contribution of the complementary hologram, extension of the hologram to the full sphere by using the measured symmetries[5], low-pass filtering[8] and, finally, multiple energy reconstruction by the Helmholtz–Kirchhoff transformation modified according to Barton[7].

The results of the measurements and analysis are shown in Fig. 1. The hologram measured at 17.9 keV incident energy is depicted after background subtraction (Fig. 1, top left): the different symmetry points of the hologram and the standing-wave line pattern (the narrow dark and bright lines) can be readily identified. We used these to extend the hologram[5] to those areas that could not be measured (shaded in grey) (another seven holograms have similar features and comparable quality).

In the final three-dimensional real-space image, the oxygen atoms are evident (Fig. 1, bottom left) (only a limited part of the reconstruction is shown for clarity). The precise measurement of these holograms allowed us not only to reconstruct the oxygen atoms, but also to image the much more distant nickel atoms up to the seventh coordination shell. This means that there are about 150 atoms in the volume imaged holographically. The (100) atomic plane is shown with distant atoms in Fig. 1, bottom right, illustrating the high and isotropic resolution of the measurement.

Holograpic imaging might be extended to systems in which long-range translation periodicity is not present and where X-ray diffraction or extended X-ray absorption fine structure cannot be used efficiently, such as for quasicrystals or single molecules. In quasicrystals, we could see atomic decorations directly. A combination of fourth-generation free-electron laser-type X-ray sources with holographic imaging and reconstruction should lead to the structural determination of single molecules, viruses and other minute systems that cannot be crystallized.

Miklós Tegze*, Gyula Faigel*, Stefano Marchesini†, Michel Belakhovsky†, Olivier Ulrich†

**Research Institute for Solid State Physics and Optics, 1525 Budapest, PO Box 49, Hungary*
†Service de Physique des Matériaux et Microstructures, Département de Recherche Fondamentale sur la Matière Condensée, CEA Grenoble, 17 rue des Martyrs, 38054 Grenoble, France

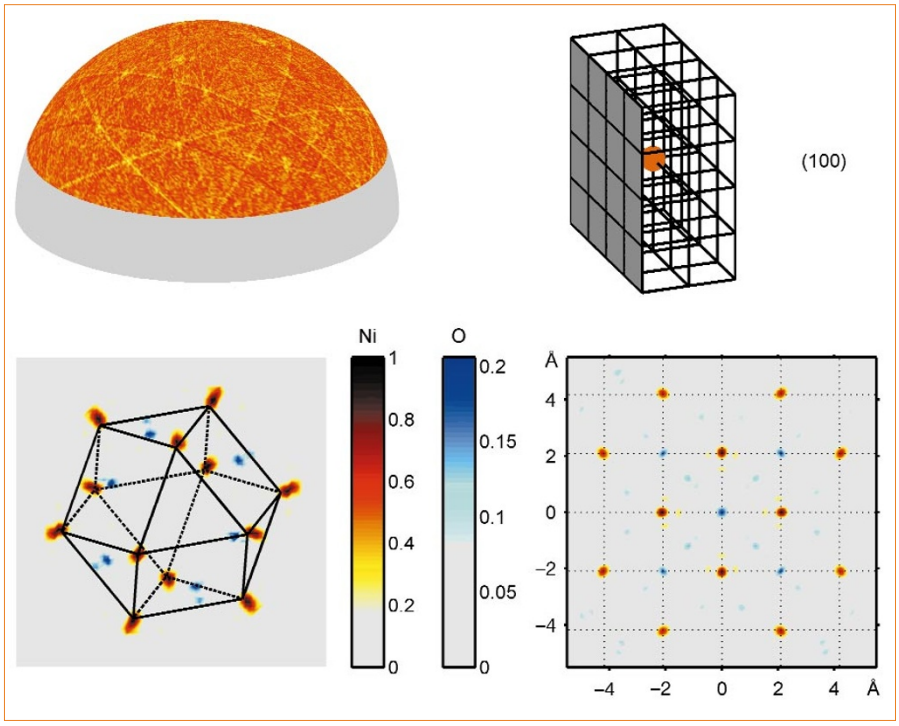

Figure 1 Holographic imaging of atoms in a nickel oxide crystal. Top left, the hologram of NiO is shown in three dimensions on a spherical surface that extends to the half sphere. Shaded grey area indicates the part of the full holographic information that could not be measured. Bottom left, three-dimensional real-space image of atoms within a sphere of radius 6 Å. Oxygen atoms are blue and nickel atoms are red. Bottom right, (100) atomic plane. Atoms can be reconstructed over large distances with isotropic resolution. Top right, for clarity it is also shown how the reconstructed plane relates to the lattice and to the central atom. The colour scale is proportional to the holographic reconstructed intensity.

1. Szöke, A. in *Short Wavelength Coherent Radiation: Generation and Applications* (eds Attwood, D. T. & Boker, J.) 361–367 (AIP Conf. Proc. no. 147, American Institute of Physics, New York, 1986).
2. Tegze, M. & Faigel, G. *Nature* **380,** 49–51 (1996).
3. Gog, T. *et al. Phys. Rev. Lett.* **76,** 3132–3135 (1996).
4. Faigel, G. & Tegze, M. *Rep. Progr. Phys.* **62,** 355–392 (1999).
5. Tegze, M., Faigel, G., Marchesini, S., Belakhovsky, M. & Chumakov, A. I. *Phys. Rev. Lett.* **82,** 4847–4851 (1999).
6. Len, P. M., Thevuthasan, S., Fadley, C. S., Kaduwela, A. P. & Van Hove, M. A. *Phys. Rev. B* **50,** 11275–11278 (1994).
7. Barton, J. J. *Phys. Rev. Lett.* **67,** 3106–3109 (1991).
8. Tegze, M. & Faigel, G. *Europhys. Lett.* **16,** 41–46 (1991).

Neurophysiology

Good memories of bad events in infancy

If a helpless newborn infant does not form an attachment to its care-giver, even an abusive one, its chances of survival diminish, so evolution should strongly favour attachment by the infant, regardless of the quality of care-giving[1]. As a part of the brain called the amygdala is critical for learned fear in adult animals[2–4], we investigated whether the development of learned avoidance behaviour could be delayed by late maturation of amygdala function. We found that very young rat pups exposed to various odours associated with shock treatment learn an approach response to that odour, whereas older pups learn odour

avoidance. We show that the origin and development of learned odour-avoidance behaviour is associated with enhanced neural responses in the amygdala during odour-shock conditioning.

Attachment in infant rats is learned predominantly postnatally, relying mainly on the olfactory system — learned odour cues are necessary for successful nipple attachment and for orientation to the mother and litter[5]. As a model for early attachment to an abusive care-giver, we used odour–shock pairings in neonatal rats (fear-conditioning paradigm[6,7]) that result in odour approach by very young rats but an odour aversion in older rats. Pups were trained in a classical-conditioning paradigm in which odour is paired with shock, or they were exposed only to the odour. Four hours after training, pups were tested for relative odour preference in a two-odour choice test.

Figure 1a shows that the conditioning of approach to odours paired with aversive shock occurs during a period that ends before postnatal day (PN) 10. Pups trained after this sensitive period learn to avoid odours paired with shock (analysis of variance (ANOVA), conditioning group × postnatal age, $F_{2,54} = 9.29$, $P < 0.001$; Fisher post-hoc tests indicate that the PN9 paired pups are significantly different from the PN10 and PN11 pups, $P < 0.01$). This striking difference in the learned behavioural responses of PN9 and older pups occurs despite their similar responses to shock (vocalization, vigorous physical response, wall climbing[6,7]; Fig. 1c, d). Furthermore, both PN9 and PN10 pups try to escape from the shock (results not shown).

Once acquired, a learned odour-approach response to odours paired with shock before PN10 continues to be expressed as an approach even in older pups that are capable of learning an aversion (good memory of a bad event). We trained pups with odour–shock pairings on PN9 and tested them after either 4 or 24 hours (on PN10). As shown in Fig. 1b, pups trained on PN9 and tested either on PN9 or PN10 showed a relative odour preference for the odour paired with shock (ANOVA, main effect of conditioning group, $F_{1,33} = 17.94$, $P < 0.001$; Fisher post-hoc tests indicate that each paired group is significantly different from each control group, $P < 0.01$).

To determine the role of the amygdala in the differential response to odour–shock training, we injected PN8 and PN12 pups with ^{14}C-2-deoxyglucose and subjected them to a 45-min odour–shock or control classical-conditioning procedure. Amygdala uptake of labelled 2-deoxyglucose was expressed relative to uptake in the corpus callosum, which did not vary across conditioning groups. The relative uptake by the amygdala was higher in PN8 pups than in PN12 pups, but did not vary with conditioning group in PN8 pups. However, it was significantly enhanced in PN12 pups trained in odour–shock pairings compared with control pups (ANOVA, training group × age interaction, $F_{2,35} = 3.37$, $P < 0.05$; post-hoc Fisher tests revealed PN12 paired pups were significantly different from both PN12 control groups, $P < 0.05$).

Our results show that the appearance of a learned odour aversion using this conditioning paradigm originates with the initial appearance of an aversive conditioning-induced enhancement of neural activity within the amygdala. We cannot infer a causal connection between amygdala development and ontogeny of avoidance conditioning, however. In fact, illness-induced odour aversions and conditioned taste aversions can be induced in pups during their first postnatal week, although illness-induced aversions may involve a different mechanism from fear conditioning[7–9]. Nonetheless, our results indicate that a unique behavioural[10] and neural response to aversive conditioning may exist in helpless newborns during a time when aversion to a care-giver could be fatal.

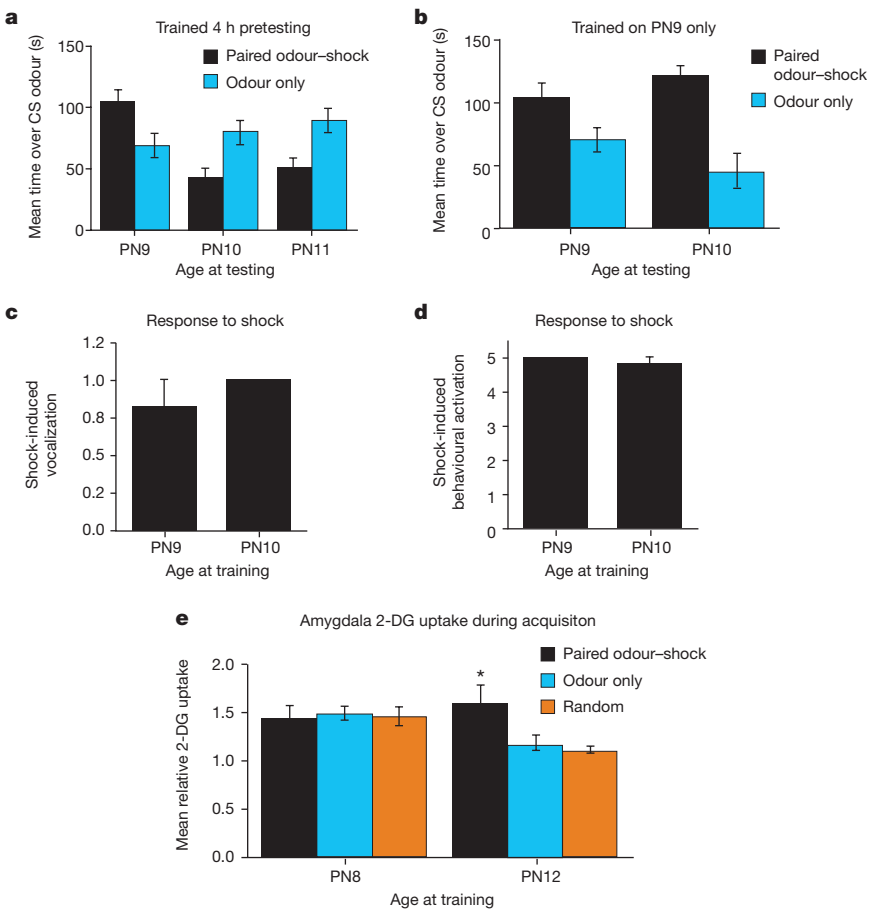

Figure 1 Ontogeny of learned odour aversions corresponds to the ontogeny of amygdala activation. **a,** Postnatal-day (PN)-9 pups trained with paired odour–shock demonstrated a subsequent odour preference compared with PN9 controls. Older pups showed learned odour aversions (*n*, 8–12 per group). **b,** Pups trained on PN9 continued to show an odour preference for an odour paired with shock, even at an age when they could learn an odour aversion ($n = 8$). **c,d,** PN9 pups find shock as aversive as PN10 pups (as measured by shock-induced vocalizations, in **c**, and behavioural activation in **d**; *n*, 5–6). **e,** Association of odour and shock produces enhanced neural activity within the amygdala of PN12 pups compared to controls, whereas the same training does not differentially affect amygdala activity in PN8 pups (*n*, 6–8). CS, conditioning stimulus; 2-DG, 2-deoxyglucose.

Regina M. Sullivan, Margo Landers, Brian Yeaman, Donald A. Wilson
Department of Zoology, University of Oklahoma, Norman, Oklahoma 73019, USA
email: rsullivan@ou.edu

1. Bowlby, J. *Attachment* Vol. 1 (Basic Books, New York, 1969).
2. Fanselow, M. S. & LeDoux, J. E. *Neuron* **23,** 229–232 (1999).
3. Davis, M. in *The Amygdala: Neurobiological Aspects of Emotion, Memory and Mental Dysfunction* (ed. Aggleton, J. P.) 255–305 (Wiley-Liss, New York, 1992).
4. Aggleton, J. P. *The Amygdala: Neurobiological Aspects of Emotion, Memory and Mental Dysfunction* (Wiley-Liss, New York, 1992).
5. Wilson, D. A. & Sullivan, R. M. *Behav. Neurobiol.* **61,** 1–18 (1994).
6. Camp, L. L. & Rudy, J. *Dev. Psychobiol.* **22,** 25–42 (1989).
7. Haroutunian, V. & Campbell, B. A. *Science* **205,** 927–929 (1979).
8. Chambers, K. C. *Annu. Rev. Neurosci.* **13,** 373–385 (1990).
9. Kucharski, D. & Spear, N. E. *Dev. Psychobiol.* **17,** 465–479 (1984).
10. Hunt, P. S. & Campbell, B. A. in *Learning, Motivation and Cognition* (eds Bouton, M. E. & Fanselow, M. S.) 53–74 (American Psychological Association, Washington DC, 1997).